J|A|C|S
ARTICLES
Published on Web 11/10/2007

The Role of Selection Pressure in RNA-Mediated Evolutionary Materials Synthesis

Stefan Franzen,*[,†,§] Marta Cerruti,[†,§] Donovan N. Leonard,[‡,§] and Gerd Duscher[‡]

Contribution from the Department of Chemistry, Department of Materials Science and Engineering, and W.M. Keck Center for RNA-mediated Evolutionary Materials Synthesis, North Carolina State University, Raleigh, North Carolina 27695

Received August 11, 2007; E-mail: stefan_franzen@ncsu.edu

Abstract: Evolutionary materials synthesis is a provocative concept that has the potential for the discovery of novel compounds ranging from drugs to inorganic materials. RNA-mediated evolutionary materials synthesis requires aqueous solvent of moderate ionic strength, water-soluble precursors, and an appropriately designed selection pressure. Throughout the selection process, the RNA must be folded, stable, and accessible once it has bound to a target, catalyzed a chemical reaction, or templated formation of a structure. Subsequently, the RNA must be accessible to permit reverse transcriptase to create DNA copies for amplification. A well-designed selection will generate RNAs that can favor growth of a particular crystal habit or catalyze a specific reaction pathway. In this study we rigorously test the assumptions, procedures, and results of the only published example of an RNA-mediated evolutionary materials synthesis. The proof that a particular RNA sequence is responsible for a novel material synthesis must be established by control experiments as outlined in the present study. Furthermore, the product of nanoscale synthesis must be studied using state-of-the-art characterization methods to determine that selection pressure is exerted according to design. Herein, we demonstrate the use of advanced electron microscopy to determine chemical composition and structure as a critical step in analysis of the success of a selection. We conclude that RNA selections should not be carried out in binary solvent systems, such as tetrahydrofuran (THF) and water. A specific example, which is not consistent with rigorous selection of functional RNAs or RNA cognates, is provided by the precipitation of the water-insoluble precursor, tris(dibenzylideneacetone) dipalladium(0) $Pd_2(DBA)_3$.

Introduction

The capability to evolve molecular compounds in the laboratory is based on a design for selection pressure that mimics natural selection. Whereas natural selection is based on the ability of living organisms to reproduce, selection pressure is achieved in the laboratory by retrieving an active sequence from a randomized pool following a chemical or physical transformation under an artificially imposed constraint. Life on earth most likely started with RNA as the central information repository and catalyst. Evolutionary chemistry can be based on RNA-based ribozymes,[1] directed evolution of protein enzymes or abzymes (anti-body enzymes)[2] that can be selected for new functions as catalysts, artificial ligands, or receptors. As more complicated function and greater chemical diversity is contemplated, genetic algorithms[3] have helped to move combinatorial chemistry into the realm of evolutionary chemistry as well. Artificial strategies for the synthesis of inorganic materials that employ RNA as a catalyst or templating agent are a recent innovation.[4,5] The central challenge to evolutionary chemistry is to design effective selections that apply pressure on the sequence space that causes only a small fraction of the sequences to survive on each synthetic cycle.

An RNA sequence known as RNA Pd 17 was reported[4] to create metallic palladium hexagons with an edge length in the micrometer range from the organometallic starting material $Pd_2(DBA)_3$ in aqueous solution. The premise of the research[4,5] is that 5-(carboxamide-4-pyridylmethyl) uridine-modified RNA sequences capable of forming Pd nano- and microparticles from $Pd_2(DBA)_3$ can be discovered by the process known as **s**ystematic **e**volution of **l**igands by **ex**ponential enrichment (SELEX). The modified RNA can also be called an RNA cognate. The original SELEX process selects for the ability of an RNA aptamer to bind to a target[6] out of a pool of greater than 10^{12} random sequences. The selection of RNA cognate catalysts for organic reactions is more demanding than binding to a target.[1] The RNA must catalyze a reaction and remain bound to the target/product so that it can be retrieved for amplification. For example, in the design of a selection for an RNA enzyme

[†] Department of Chemistry.
[‡] Department of Materials Science and Engineering.
[§] W.M. Keck Center for RNA-mediated Evolutionary Materials Synthesis.

(1) Tarasow, T. M.; Tarasow, S. L.; Eaton, B. E. *Nature* **1997**, *389*, 54−57.
(2) Jackson, D. Y.; Jacobs, J. W.; Sugasawara, R.; Reich, S. H.; Bartlett, P. A.; Schultz, P. G. *J. Am. Chem. Soc.* **1988**, *110*, 4841−4842
(3) Weber, L. *Drug Discovery Today* **1998**, *3*, 379 385
(4) Gugliotti, L. A.; Feldheim, D. L.; Eaton, B. E. *Science* **2004**, *304*, 850−852.
(5) Gugliotti, L. A.; Feldheim, D. L.; Eaton, B. E. *J. Am. Chem. Soc.* **2005**, *127*, 17814−17818.
(6) Tuerk, C.; Gold, L. *Science* **1990**, *249*, 505−510.

for the Diels−Alder reaction, retrieval of the RNA can be accomplished by tethering the RNA to one of the reactants, with a selection tag (e.g., biotin) to a second reactant.[1] Thus, RNA catalyzes bond formation that unites the RNA itself to a biotin molecule. Selection takes place when the RNA−biotin product binds to streptavidin and is isolated from inactive RNA sequences. The cycle is completed by reverse transcription of the selected active sequences into DNA that becomes the template for a new round of RNA selection. In order to select for an RNA sequence that mediates the creation of new inorganic materials, there must be a chemical transformation, crystallization, or aggregation of the precursor mediated by the RNA, and the RNA must remain bound to the inorganic product[7] so that it can be retrieved and amplified. As a templating process, RNA-mediated materials synthesis is analogous to phage display approaches.[8] Two examples of RNA-mediated formation of CdS and PbS nanoparticles have been recently reported.[7,9]

The report of metal−metal bonds in crystalline, micrometer-sized hexagonal palladium (Pd) particles describes the mediation by pyridine-modified RNA cognates in an aqueous solution of $Pd_2(DBA)_3$.[4] In order to create crystalline Pd microparticles from the precursor molecules, $Pd_2(DBA)_3$, the active RNA sequences must mediate the reaction [n $Pd_2(DBA)_3 \rightarrow (Pd-Pd)_n$ (metal) + 3n DBA] in water, template or catalyze particle formation, and remain bound to the product. In such a selection, one would harvest the active RNA sequences by collecting the crystalline Pd particles as claimed in refs 4 and 5. However, one must confront the incompatibility between the water-insoluble $Pd_2(DBA)_3$ precursor and the folding requirements of RNA in aqueous solution. In both RNA-mediated material synthesis and in biology, RNA structure is crucial for effective catalysis and information storage, and that structure is maintained only in buffered aqueous solutions as far as we know at the present time. RNA selections for organic reactions have led to the use of binary solvent mixtures of up to 10% ethanol.[1] While the field of enzymology has been widened to include enzymes that function in pure organic solvents,[10] the polyanionic nature of RNA and concomitant requirement of ions for structural definition has thus far precluded any similar demonstration in the world of nucleic acids.

The concept of RNA-mediation of metal−metal bond formation[4,5] must be rigorously tested to prove that the selection pressure is targeting the intended properties, the RNA is functional, and the product is indeed metallic. The solubility of precursors and the chemical nature of the precursor interaction with RNA must be established as part of the design of the selection. Control experiments and nanoscale characterization to determine crystalline nature and chemical composition of precipitates are an integral part of this study and should be part of any study to discover new materials by an evolutionary process.

Results

We were interested in the mechanism whereby cognate RNA Pd 17 catalyzes or templates the formation of the Pd nano- and microparticles.[4,5] During the course of structural studies on the reported crystalline Pd hexagonal particles,[4] we discovered that RNA Pd 17 is not required for the formation of the hexagonal particles. Working in collaboration with the authors of refs 4 and 5, and using their reagents, we observed that precipitates formed rapidly when experiments were performed repeating the protocols of ref 4. Specifically, when 5%THF/H_2O solutions were prepared using diethylpyrocarbonate (DEPC) water, purified tetrahydrofuran (THF), and freshly ordered $Pd_2(DBA)_3$ from Strem Chemicals, a precipitate formed within 20 min in the presence of freshly prepared RNA Pd 17. Control experiments in 5% THF/H_2O without RNA Pd 17 yielded immediate precipitation. Figure 1A shows a close-up of the precipitate formed in the 5%THF/H_2O solution with no RNA present. The image shows the effect of addition of saturated THF, reported as 8 mM in ref 4, without stirring or shaking. The aqueous solvent condition reported in ref 4 could not be duplicated because $Pd_2(DBA)_3$ is completely insoluble in water.[11,12]

Since the conditions described in ref 4 and 5 are not conducive to a controlled selection of functional RNAs due to the observed rapid precipitation rates, we investigated conditions that could possibly have been used to obtain the reported solutions of $Pd_2(DBA)_3$. $Pd_2(DBA)_3$ was added to binary mixtures of THF and water ranging from 5% THF/ H_2O to pure THF. Turbid suspensions and precipitates were observed to form rapidly in any solution with a volume percentage of less than 50% THF (Figure 1B). These results were independently verified in two other laboratories (see Acknowledgment).

Figure 1. (A) Close-up picture of 400 μM $Pd_2(DBA)_3$ in 5% THF/H_2O showing the black precipitate formed 2 min after the preparation of the solution. (B) Picture of suspensions of 400 μM $Pd_2(DBA)_3$ in binary mixtures of THF and water. (1) 5% THF/H_2O; (2) 30% THF/H_2O; (3) 50% THF/H_2O; (4) 70% THF/H_2O; (5) 100% THF.

(7) Ma, N.; Dooley, C. J.; Kelley S. O. *J. Am. Chem. Soc.* **2006**, *128*, 12598−12599.
(8) Mao, C. B.; Solis, D. J.; Reiss, B. D.; Kottman, S. T.; Sweeney, R. Y.; Hayhurst, A. L.; Georgiu, G.; Iverson, B.; Belcher, A. M. *Science* **2004**, *303*, 213−217.
(9) Kumar, A.; Jakhmola, A. *Langmuir* **2007**, *23*, 2915−2918.
(10) Akiyama, A.; Bednarski, M.; Kim, M. J.; Simon, E. S.; Waldmann, H.; Whitesides, G. M. *Chemtech* **1988**, *18*, 627−634.
(11) Rodman, D. L.; Carrington, N. A.; Xue, Z.-L. *Talanta* **2006**, *70*, 426−431.
(12) Materials Safety Data Sheet, CAS 52409-22-0.

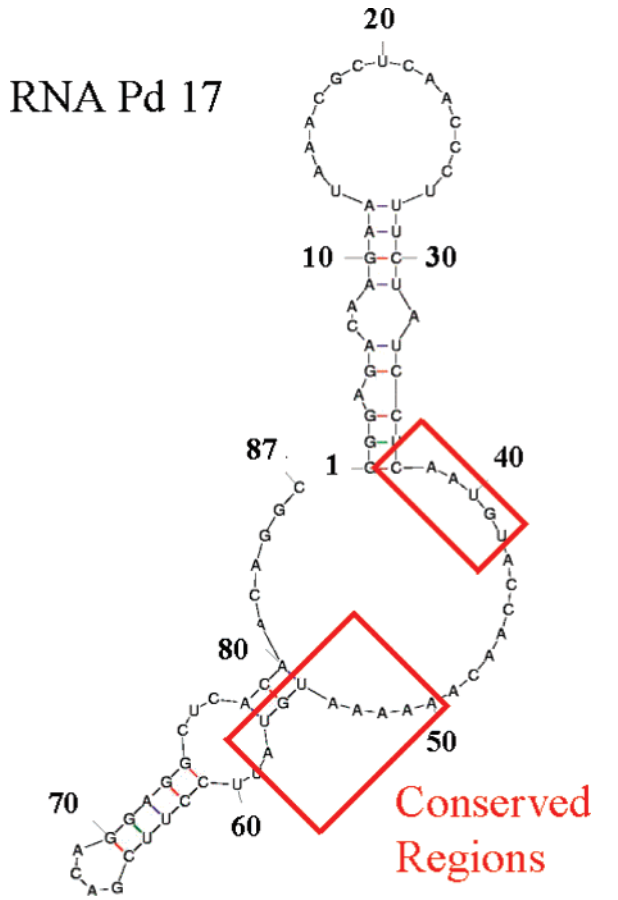

Figure 2. Lowest-energy structure of RNA Pd 17 determined by MFOLD. Four structures were found that all had similar isolated A-helices with at most five consecutive canonical base pairs and 19 or less total base pairs. The conserved regions are contained within the red boxes.

Given the low water solubility of the precursor $Pd_2(DBA)_3$ and concomitant requirement for the addition of an organic solvent, THF, to water, it is worth considering the effect of this binary solvent mixture on the structure of RNA Pd 17. Ordinarily, one would avoid even modest concentrations of organic solvents, such as THF, when working with RNA in order to avoid denaturation.[13] However, RNA denaturation (vide infra) can only be invoked once a folded structure has been established. To this end, we analyzed the secondary structure of the RNA using the program MFOLD[14] as shown in Figure 2. MFOLD predicts at most 19 base pairs in the 87-mer. It is most significant that the two conserved regions, CAAUGU and AAAAAUGUA, identified in refs 4 and 5, are stabilized by no base pairs and three base pairs, respectively (see red box in Figure 2). The lack of base pairing in the conserved region is not consistent with a folded structure in the part of the sequence required for function. Concern for the nature of the folded state was heightened by the fact that the published procedure in refs 5 and 15 calls for selection of the RNA cognates in 5% THF and distilled H_2O without the addition of any ions that would facilitate RNA folding. A standard RNA folding buffer would contain a minimum of 1 mM $MgCl_2$ and 100 mM NaCl.[16,17] Without electrostatic screening by ions during the selection, the mutual repulsion of the charged groups on the phosphodiester backbone would further destabilize RNA Pd 17. The pendant pyridinyl groups of modified RNA have a pK_a of 5.3 and therefore are neutral at pH 7.0. Based on these considerations, RNA Pd 17 has little or no folded structure and therefore no structured region surrounding the conserved nucleotides under the conditions of the selection.

The denaturation of folded RNA will abolish its function. To this end the denaturation of RNA Pd 17 was reported[13] as a control experiment in the presence of THF. It was reported that no hexagonal microparticles formed when the RNA was denatured in pure THF.[13] In order to test the role of the denaturation of surface-attached RNA Pd 17 reported in ref 13, we used optical microscopy to observe the effect of neat THF on surface-bound hexagonal particles formed in the presence of RNA Pd 17. These experiments showed that the hexagonal particles were *dissolved* by neat THF. This was observed in sequential measurements on an immobilized microscope slide using an optical microscope. First, a hexagon was identified in the field of view of the microscope. Subsequently, the immobilized slide was rinsed with THF. Then the slide was reexamined to confirm that the hexagon in the original field of view was no longer present. To verify that the process was not a simple rinsing of the hexagon, the dissolution of the hexagonal particles was also observed in real time under a Zeiss LSM 5 Pascal confocal microscope. Given that the protocol for denaturation of RNA in the control experiment in ref 13 calls for formation of a hexagon in neat THF at 55 °C, we conclude that the most reasonable explanation for the observed lack of hexagonal particles is not that the RNA was denatured, but rather that the hexagonal particles were dissolved by the THF. Moreover, if the hexagonal microparticles were composed of metallic Pd as claimed,[4,5,13] they would not dissolve in an organic solvent such as THF as observed. These observations are consistent with hexagonal particles composed of $Pd_2(DBA)_3$, but not consistent with the claim that they are metallic Pd.[4,5,13]

In order to fully understand composition and structure of these particles, we studied the precipitates obtained in the THF/H_2O mixtures using analytical electron microscopy. The morphology of the particles was determined by field emission scanning electron microscopy (FESEM) and bright-field (BF) transmission electron microscopy (TEM) (Figure 3,A and B). The hexagon-shaped precipitates formed by simple evaporation of the $Pd_2(DBA)_3$ reagent from THF solution onto a conductive ITO surface are shown in the secondary electron (SE) micrograph of Figure 3A. The features observed in the SE micrographs (Figure 3A) show charging effects indicative of an electrically insulating material on the conductive ITO surface. Figure 3B shows a BF TEM micrograph of particles formed in a 50% THF/H_2O suspension of 400 μM $Pd_2(DBA)_3$. The hexagonal particles obtained in the presence of RNA Pd 17 reported in ref 4 are shown in Figure 3C. The morphology of these hexagonal particles is identical to that of the particles formed in control experiments without any RNA (Figure 3, A and B). Similar particles have been observed from a variety of THF/H_2O binary solvent mixtures, together with features such as rods and cubes. In solutions with THF percentage between

(13) Liu, D.; Gugliotti, L. A.; Wu, T.; Dolska, M.; Tkachenko, A. G.; Shipton, M.; Feldheim, D. L.; Eaton, B. E. *Langmuir* **2006**, *22*, 5862−5866.
(14) Zuker, M. *Science* **1989**, *244*, 48−52.
(15) Gugliotti, L. Ph. D. Thesis, North Carolina State University, 2006, 51−52.
(16) Thirumalai, D.; Lee, N.; Woodson, S. A.; Klimov, D. K. *Ann. Rev. Phys. Chem.* 2001, *52*, 751−762.
(17) Misra, V. K.; Draper, D. E. *J. Mol. Biol.* **2002**, *317*, 507−521.

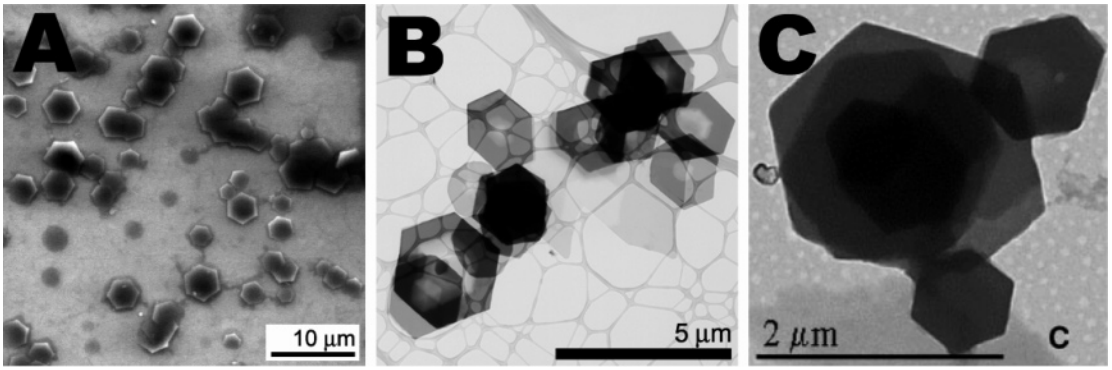

Figure 3. Comparison of hexagonal particles synthesized with and without RNA Pd 17. (A) Particles made by evaporation of $Pd_2(DBA)_3$ from 8 mM THF solution on ITO. (B) Particles resulting from 400 μM $Pd_2(DBA)_3$ dissolved in 50% THF/H_2O colloidal suspension deposited on a lacey carbon grid (binary mixture #3 in Figure 1A). (C) Reproduction from ref 4. Hexagonal-shaped particles synthesized in the presence of RNA Pd 17 in aqueous solvent.

30% and 100%, hexagonal particles represented the vast majority of the particles found. A detailed analysis of the different particle morphology observed in relationship with THF/H_2O solvent composition will be described elsewhere.

Quantitative energy dispersive spectroscopy (EDS), 30-kV and 200-kV scanning TEM (STEM), and electron energy-loss spectroscopy (EELS) were used to ascertain the chemical composition of the hexagonal particles. Analysis of the EELS data obtained on samples made by the authors of ref 4 and later by us in the presence of RNA Pd 17 indicates a composition of 92.5 (±12.9)% C and 6.4 (±0.8)% Pd by atom. A similar composition (~90% C and ~10% Pd by atom) was obtained also with 30-kV STEM/EDS shown in Figure 4 for samples prepared without RNA Pd 17. The size, morphology, and composition of the hexagons were nearly the same when prepared with or without RNA Pd 17. Both of the chemical analysis results are consistent with the atomic composition of the $Pd_2(DBA)_3$ reagent, but not with that of metallic Pd.

The atomic structure of the particles was studied using selected area electron diffraction (SAD) acquired from micrometer-sized regions of single hexagons and clusters. The observed SAD patterns were repeatedly influenced by exposure time and intensity of the 200-kV electron beam. The beam-induced dependence of SAD results indicated the hexagons were not pure Pd metal. Three stages were identified according to beam exposure time. Stage 1, shown in Figure 5, can be observed only within the first 10 s of beam exposure. In stage 1, a six-fold symmetric spot pattern with nanometer-scale lattice spacings was observed (Figure 5B). The lattice spacings, from indexing the lower index spots, were found to be 1.106 (±0.004) nm and 0.642 (±0.001) nm, respectively, with angles between planes measuring 60 (±0.1)°. Lattice spacings in the ~1-nm range clearly indicate molecular rather than atomic packing. The available X-ray crystal structures of $Pd_2(DBA)_3$ contain either a CH_2Cl_2 or a C_6H_6 solvent molecule. Both structures have a triclinic unit cell that resembles a distorted trigonal unit cell.[18] The data in Figure 5B are consistent with $Pd_2(DBA)_3$ crystals in a trigonal space group with unit cell lengths similar to those reported[13] for crystalline $Pd_2(DBA)_3$. After approximately 10 s, the "critical dose" was surpassed, and radiation damage occurred in these carbon-based samples.[19] SAD results obtained in stage 2 and shown in Figure 6 yielded diffuse rings indicative

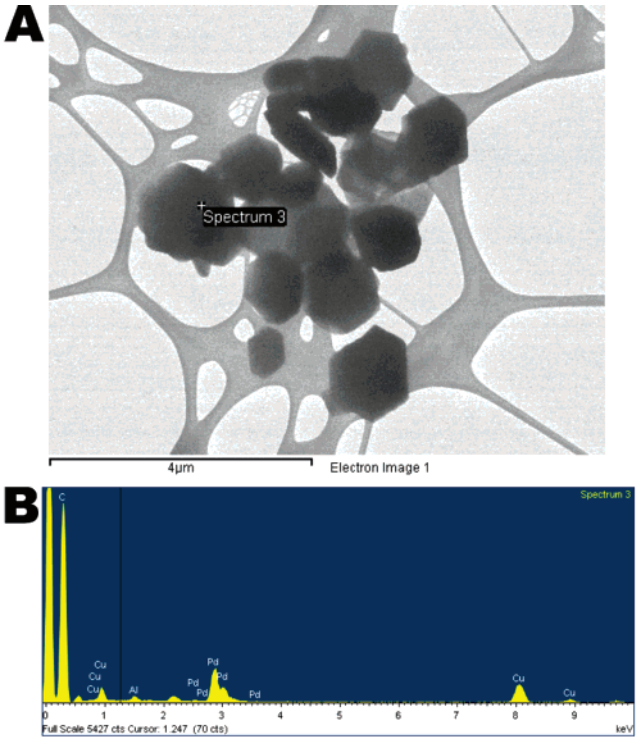

Figure 4. Diffraction contrast micrograph and EDS spectra of hexagonal particles obtained from 50% THF/H_2O solution without RNA mediation. (A) Diffraction contrast micrograph obtained by LV-STEM. (B) X-ray spectra were acquired by EDS to determine the chemical composition of the hexagonal cluster shown in A. No significant carbon signal was excited from the lacey carbon film because the EDS was acquired from a region of the sample suspended over vacuum. The faceted hexagonal structures sampled from the micrometer-sized cluster were composed of mostly carbon with some Pd present as indicated by the relative intensities of the X-ray peaks. The Cu and Al X-ray peaks present in the spectra are emitted from the Cu TEM grid and Al clamp used to fix the TEM grid into the sample holder.

of an amorphous material. Further beam damage was evident after 5 or more minutes under the electron beam as shown in Figure 7. In stage 3, small regions approximately 5 nm in diameter, appeared in the $Pd_2(DBA)_3$ hexagons as shown in Figure 7B. These regions were observed prior to stage-3 electron beam damage as shown by the comparison in Figure 7, A and B, before and after stage-3 beam damage, respectively. The SAD results in Figure 7C show a combination of diffuse rings from the amorphous $Pd_2(DBA)_3$ with stage-2 beam damage and a more defined set of diffraction rings that arise from the small

(18) Pierpont, C. G.; Mazza, M. C. *Inorg. Chem.* **1974**, *13*, 1891−1895.
(19) Egerton, R. F.; Li, P.; Malac, M. *Micron* **2004**, *35*, 399−409.

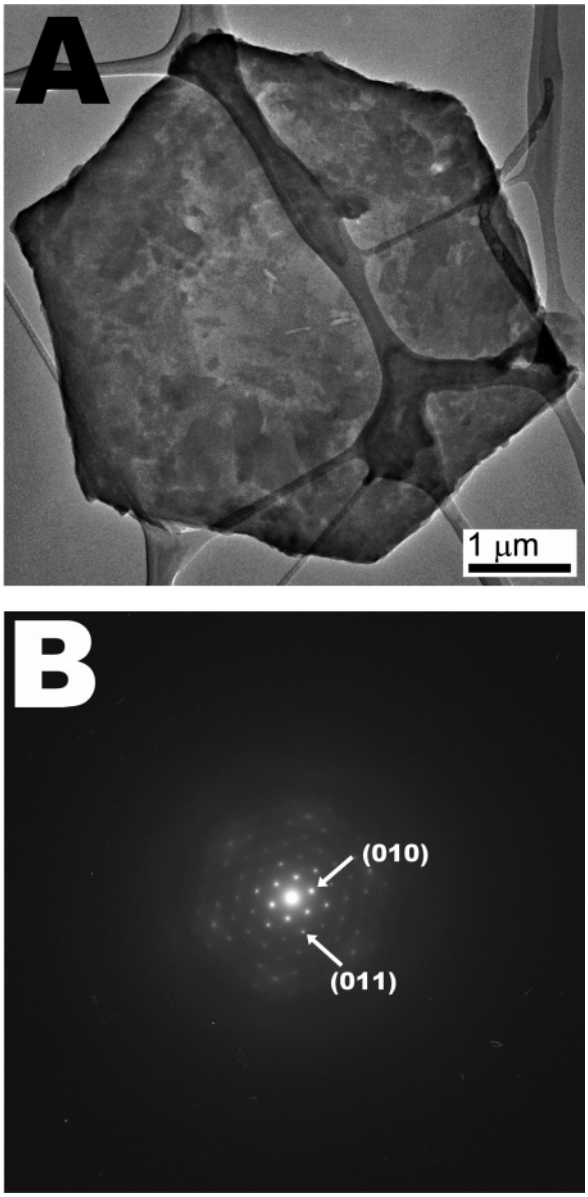

Figure 5. Observable TEM image and SAD pattern obtained within the first 10 s of beam exposure, designated as stage 1. (A) Bright-field TEM micrograph of nanostructures created from 50% THF/H_2O on a lacey carbon grid. (B) Diffraction pattern (acquired at 60-cm camera length) of corresponding feature shown in A.

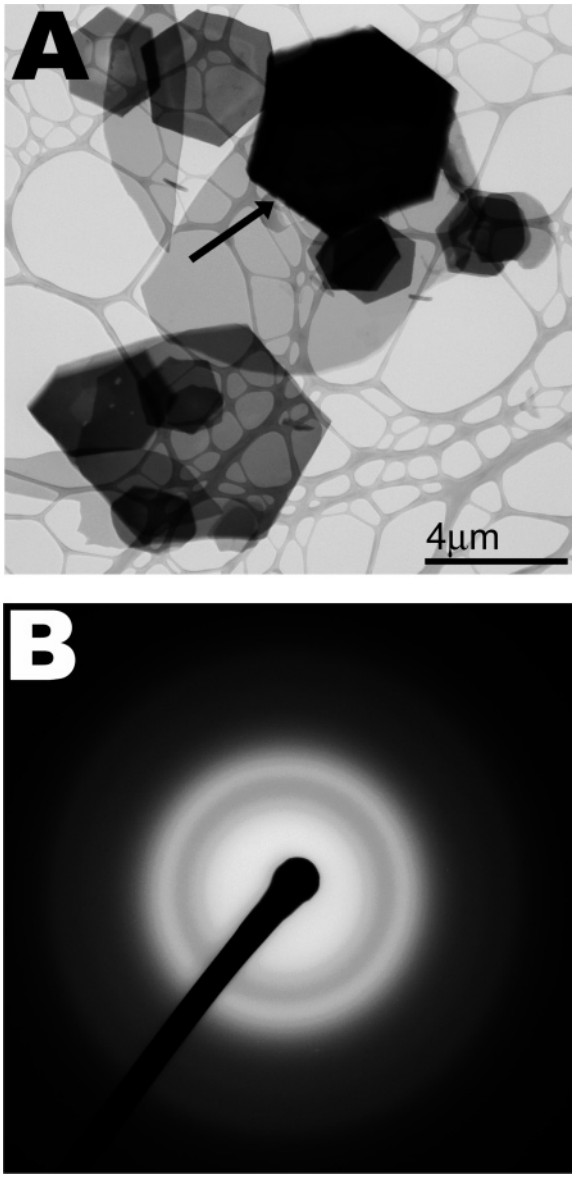

Figure 6. Observable TEM image and SAD pattern obtained after 20 s of beam exposure, but within the first 5 min, designated as stage 2. (A) Bright-field TEM micrograph of nanostructures created from 50% THF/H_2O on a lacey carbon grid. (B) Diffraction pattern (acquired at 60-cm camera length) of corresponding feature shown in A.

Pd nanoparticles formed by the stage-3 beam damage shown in Figure 7B. The 5-nm features have lattice fringes indicative of crystalline Pd that are evident in the HRTEM image as observed both by us and in ref 15. The data presented in ref 15 correctly state that the samples studied there and in ref 4 were observed in stage 3. Prolonged high electron flux damages the dibenzylidene acetone moiety and permits Pd atoms to diffuse and coalesce to form Pd nanoparticles. Each individual 5-nm Pd nanoparticle in a given hexagon may be a single crystal. However, given that the SAD region is several micrometers in diameter, the overall electron diffraction results in a polycrystalline ring pattern.

A second source of Pd metal that can give rise to SAD ring patterns was found in the as-received reagent powder from Strem Chemicals. We studied fresh $Pd_2(DBA)_3$ reagent powder the same day it arrived in our laboratory and observed nanocrystalline Pd metal impurities. Similar Pd metal impurities were also observed when $Pd_2(DBA)_3$ was dissolved in 100% THF as shown in Figure 8. These nanoparticles differed in morphology from the reported micrometer-sized hexagonal platelets and appeared as 150−200-nm crystallites (cf. Figures 8A, 5A, and 6A). The SAD results in Figure 8B are consistent with metal-bonded polycrystalline Pd with (111), (200), and (220) lattice spacings of 0.225, 0.195, and 0.137 nm, respectively. The experimental Pd−Pd bond length of 0.275 nm obtained from these values agrees exactly with the published value for metallic Pd.[20]

Discussion

Despite the potential of evolutionary approaches that use RNA cognates and RNA itself, we have significant concerns regarding the design of the initial experiments in this field. First, Pd_2-

(20) Sutton, L. E., Ed. *Table of Interatomic Distances and Configuration in Molecules and Ions*; Chemical Society: London, UK, 1965.

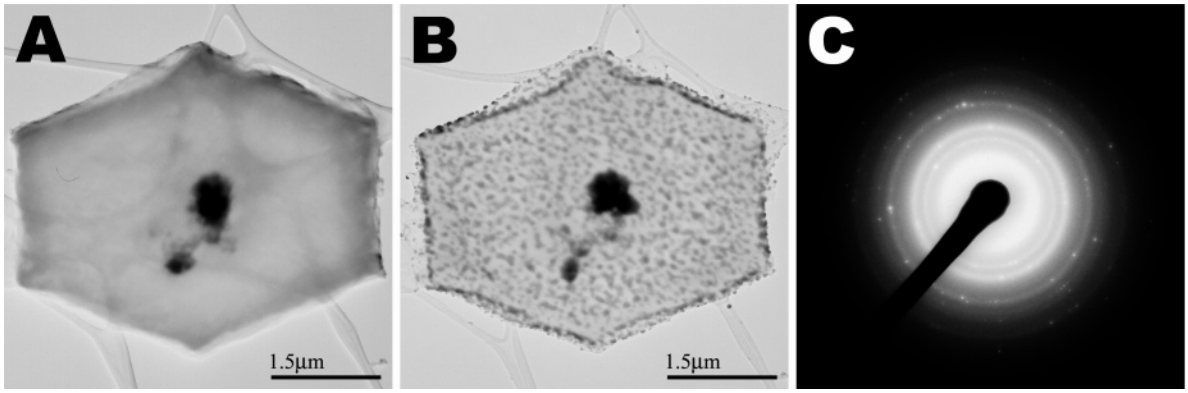

Figure 7. Observable TEM images from stages 2 and 3 showing the progressive alteration in structure and SAD pattern of the sample in stage 3. (A and B) Bright-field TEM micrograph of nanostructures created from 50% THF/H_2O on a lacey carbon grid. (A) BF TEM image obtained within the first 5 min. (B) BF TEM image obtained after 5 min. (C) Diffraction pattern (acquired at 60-cm camera length) of corresponding feature shown in B.

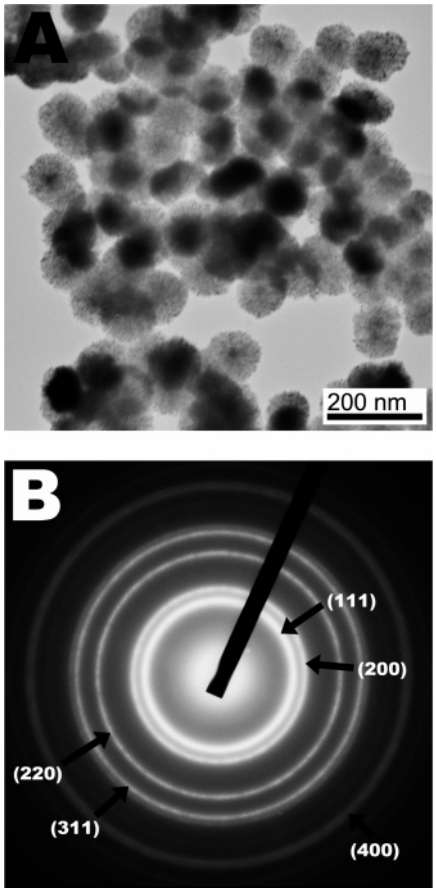

Figure 8. Observable TEM image and SAD pattern of nanoparticles plated onto the TEM grid from a 100% THF suspension of freshly purchased $Pd_2(DBA)_3$ reagent powder. (A) Bright-field TEM micrograph of nanostructures on a lacey carbon grid. (B) Diffraction pattern (acquired at 60-cm camera length) of corresponding feature shown in A.

$(DBA)_3$ does not dissolve in water as claimed in ref 4 or even 5% THF/H_2O as claimed in ref 5. Second, adequate control experiments were not performed to test whether hexagonal $Pd_2(DBA)_3$ aggregates were formed spontaneously in the absence of RNA Pd 17. Third, the selection protocol was designed without consideration of the requirements for RNA folding. There is no evidence that RNA Pd 17 has a defined secondary structure under the conditions of the selection. Fourth, the chemical composition of the hexagons was not determined correctly. Our data show that they are greater than 90% carbon by atom, i.e., the composition of the $Pd_2(DBA)_3$ starting material, and not metallic Pd. Fifth, SAD was never presented in refs 4, 5, 13, or 15. Careful application of SAD shows the stages of change in morphology that arise when the sample is subjected to a 200-kV electron beam. Sixth, the starting material apparently was not examined, which would have shown that polycrystalline spheroidal Pd nanoparticles (<200 nm) are present in the $Pd_2(DBA)_3$ received from the manufacturer. When observed by SAD without confirmation by image analysis the pattern obtained from these particles could give rise to the conclusion that Pd was formed during the RNA Pd 17 treatment rather than being a decomposition product of the starting material, $Pd_2(DBA)_3$. Based on these findings, there is clearly a need to define protocols more precisely in order to ensure that appropriate selection pressure is present under experimental conditions where RNA mediation is desired as an outcome of an evolutionary chemistry strategy.

A successful RNA-mediated evolutionary materials synthesis strategy requires solvent conditions that are compatible with RNA and with the solubility of the material used as precursor. RNA can form secondary and tertiary structures in aqueous solution. These structures can be compromised by even small quantities of organic solvent, and the ion concentration is a critical factor. Buffered water solutions are the only recommended solvents, and precursors must be water-soluble in order for selection pressure to be exerted on the RNA. The necessity of using aqueous solutions in RNA mediated evolutionary synthesis has been pointed out by the same authors of refs 4 and 5 in a recently published review.[21]

One can draw inspiration from the functions of RNA in nature. Examples of controlled self-assembly that involve mediation by RNA in nature include structures such as the ribosome[22] and spliceosome[23] and the templating of viral-coat proteins in certain RNA viruses.[24] In each of these cases, the RNA ultimately interacts with a protein structural unit, but the RNA itself is the dynamic agent of self-assembly. Of course, RNA can also act as an enzyme in biology.[25] However, the range

(21) Feldheim, D. L.; Eaton, B. *ACSNano* **2007**, *1*, 154−159.
(22) Ban, N.; Nissen, P.; Hansen, J.; Moore, P. B.; Steitz, T. A. *Science* **2000**, *289*, 905−920.
(23) Stark, H.; Luhrmann, R. *Ann. Rev. Biophys. Biomol. Struct.* **2006**, *35*, 435−457.
(24) Sherman, M. B.; Guenther, R. H.; Tama, F.; Sit, T. L.; Brooks, C. L.; Mikhailov, A. M.; Orlova, E. V.; Baker, T. S.; Lommel, S. A. *J. Virol.* **2006**, *80*, 10395−10406.
(25) Zaug, A. J.; Been, M. D.; Cech, T. R. *Nature* **1986**, *324*, 429−433.
(26) Seelig, B.; Jäschke, A. *Chem. Biol.* **1999**, *6*, 167−176.

of natural enzyme activities is limited mostly to RNA processing itself. While of critical importance to living organisms, the chemical range of this activity is limited.

RNA cognates are RNAs with modified nucleotides designed to extend the range of function. The original Diels−Alderase RNA-enzyme was discovered from a selection of RNA cognates.[1] However, more recent work has shown that nearly the same activity can be achieved using a selection based on native RNA.[26] It is important to discover the range of chemistry in native RNA. One basic motivation is that RNA cognates are expensive. However, the fundamental reason for beginning with native RNA is to understand the hypothesis that there was an RNA world that preceded the current paradigm for life.[27] A world based on RNA suggests a range of function for folded RNAs that is significantly larger than observed in living organisms today. Studies of Diels−Alderase using native RNA have elucidated new structure−function relations in RNA.[28] It would be interesting to determine the full range of function and metal binding possible in native RNA in an evolutionary strategy. These studies can use sequence information[29,30] to correlate structure with activity. The combination of genetic algorithms[3] and structure prediction[14] to develop an information science of RNA enzymes will likely contribute a great deal to the development of RNA catalysts. For example, ribonuclease-P, which was one of the first RNA enzymes discovered,[31] has been characterized in many species using sequence comparison as a tool.

While discovery of novel metal and metal oxide nanoparticles with catalytic properties is desirable from the point of view of the relative of ease of selection, the templated growth of such nanoparticles by RNA or RNA cognates is difficult to prove. Any nanoparticle must start as a cluster, and so it is interesting to consider the possibility that RNA may function as a metalloenzyme[1] with features that resemble metalloproteins. The goal of discovering new catalysts[32] may still be achieved using RNA mediation, but by analogy with protein metalloenzymes a high level of activity can be achieved with relatively small metal clusters or organized metal ions in a three-dimensional structure. Furthermore, when considering RNA as a metalloenzyme, one must recognize that ions are a double-edged sword. The ions can bind to the RNA to provide structure; however, they can also cleave RNA and destroy its structure. Regardless of the strategy chosen for selection, it is essential to include structural analysis at an early stage in the process to verify that the selected sequences indeed have a structure. The tools for analysis of RNA are now well developed[14,28−30] so that there are many checks that can be used to verify that the RNA is folded.

Conclusion

We have studied the report of RNA-mediated formation of Pd nanoparticles in order to provide further insight into the design of useful selections. We have concluded that RNA selections are not compatible with organic solvents or water-insoluble precursors. The lack of RNA structure and chemical incompatibility with RNA functional groups in mixed solvents reduces the probability of selection of sequences that are active for interaction with growing crystals or catalysis of chemical reactions. We have also shown that advanced electron microscopy can provide crucial nanoscale information on the composition and structure of materials formed in a selection. For this reason, analysis tools should be an integral part of any investigation providing the basis for experimental design in successive selection cycles. It is our hope that this study will serve to direct the field toward chemical processes that are compatible with the properties of RNA.

Acknowledgment. This study was funded by the W.M. Keck foundation. We thank Dr. Konrad Jarausch and Hideo Naito of Hitachi High Technologies America, Inc., Electron Microscope Division, Pleasanton, CA 94588, for the use of the HD 2300 STEM and the Gatan Enfina EELS spectrometer. We thank Montana Childress and Prof. Daniel Nocera of Massachusetts Institute of Technology and Drs. Chinta Reddy, Venkat Reddy, and Prof. John Verkade of Iowa State University for independently verifying the solubility studies of $Pd_2(DBA)_3$ in binary mixtures of THF and H_2O. RNA Pd 17 isolates were prepared in the laboratory of Dr. Dan Feldheim and Bruce Eaton, whom we thank for cooperation in the initial phase of this study.

Supporting Information Available: Descriptions of experimental methods used in sample preparation and conditions for electron microscopy measurements. This material is available free of charge via the Internet at http://pubs.acs.org.

JA076054R

(27) Gilbert, W. *Nature* **1986**, *319*, 618−618.
(28) Amontov, S.; Jäschke, A. *Nucleic Acids Res.* **2006**, *34*, 5032−5038.
(29) Brown, J. W. *Nucleic Acid Res.* **1999**, *27*, 314−314.
(30) Tippmann, H. F. *Briefings Bioinf.* **2004**, 5, 82−87.
(31) Westheimer, F. H. *Nature* **1986**, 319, 534−536.
(32) Feldheim, D. L. *Science* **2007**, *316*, 699−700.